BJRS
BRAZILIAN JOURNAL OF RADIATION SCIENCES

doi.org/10.15392/2319-0612.2026.3138
*Braz. J. Radiat. Sci.*, Rio de Janeiro
**Oct-Dec 2026, 14(4) | 01-18 | e3138**
Editor(s): Dr. (Prof.) Bernardo Maranhão Dantas
Dr. (Prof.) Alfredo L. Ferreira Filho
Me. Matheus Rebello do Nascimento
Submitted: 2026-06-01
Accepted: 2026-10-15

Original Article

# Patient-specific thyroid computational models and SIMIND Monte Carlo simulations for assessing the accuracy of $^{131}$I dosimetry in hyperthyroidism

Aman[a*], E. H.; Chain[b, c], C. Y.; Illanes[a], L. H.

[a] Departamento de Física, Facultad de Ciencias Exactas, Universidad Nacional de La Plata PC: 1900, La Plata, Argentina
[b] Departamento de Ciencias Biológicas, Facultad de Ciencias Exactas, Universidad Nacional de La Plata PC: 1900, La Plata, Argentina.
[c] Instituto de Investigaciones Fisicoquímicas Teóricas y Aplicadas (INIFTA), Consejo Nacional de Investigaciones Científicas y Técnicas (CONICET), Universidad Nacional de La Plata PC: 1900, La Plata, Argentina.

*Correspondence: enzo.aman@fisica.unlp.edu.ar

**Abstract**: The aim of this study was to use SIMIND Monte Carlo (MC) simulations together with patient-specific thyroid computational models to assess the accuracy of $^{131}$I-activity quantification from planar images and thyroid dosimetry calculations in radiopharmaceutical therapy with [$^{131}$I] sodium iodide for hyperthyroidism. The methodology integrates two components: (i) patient- specific thyroid computational models of big and medium goitre, generated by processing patient computed tomography scans with 3D Slicer Image computing software; and (ii) a virtual gamma camera created using SIMIND MC code. The modelled Picker Prism 2000 XP gamma camera was used to obtain planar images of the patient- specific thyroid computational models, in which a predefined $^{131}$I activity of 1.665 MBq was assigned to the thyroid volume, using a high-energy collimator and a distance thyroid/ detector of 5 cm, as clinically representative imaging conditions. The same acquisition parameters were used to obtain simulated planar images of the Zubal reference phantom and a calibration source, with the aim of quantification. Dosimetry calculations were based on a monocompartmental $^{131}$I biodistribution model, assuming a post- administration time of 24 hours, and an effective elimination time of 5.5 days. With the proposed methodological framework, two patient-specific thyroid computational models of goitre have been successfully implemented, yielding with SIMIND MC realistic, patient-morphed thyroid scintigraphies. Thyroid activity was quantified with 3% error for the Zubal phantom and ≤0.4% error for the patient-specific computational models, that propagated without modification to the absorbed dose values. The results showed that self-irradiation absorbed dose in the thyroid strongly depends on the thyroid mass that is considered, exhibiting dose values

SBPR
Copyright © 2026 Authors.
OPEN ACCESS
CC BY

BJRS
BRAZILIAN JOURNAL OF RADIATION SCIENCES

doi.org/10.15392/2319-0612.2026.3138
*Braz. J. Radiat. Sci.*, Rio de Janeiro
**Oct-Dec 2026, 14(4) | 01-18 | e3138**
Editor(s): Dr. (Prof.) Bernardo Maranhão Dantas
Dr. (Prof.) Alfredo L. Ferreira Filho
Me. Matheus Rebello do Nascimento
Submitted: 2026-06-01
Accepted: 2026-10-15

for the medium- goitre that doubled the values for the big goitre, and slightly varies with the nature of the computational model. The study illustrates the utility of SIMIND MC simulations together with thyroid computational models to estimate the accuracy of the dosimetry calculation that could emerge in a realistic clinical setting and to identify the influence of the image acquisition parameters and the thyroid mass in the calculation accuracy.

**Keywords:** SIMIND MC, patient- specific thyroid computational model, goitre, thyroid absorbed dose.

SBPR

Copyright © 2026 Authors.

OPEN ACCESS

CC BY

BJRS
BRAZILIAN JOURNAL OF RADIATION SCIENCES

doi.org/10.15392/2319-0612.2026.3138
*Braz. J. Radiat. Sci.*, Rio de Janeiro
**Oct-Dec 2026, 14(4) | 01-18 | e3138**
Editor(s): Dr. (Prof.) Bernardo Maranhão Dantas
Dr. (Prof.) Alfredo L. Ferreira Filho
Me. Matheus Rebello do Nascimento
Submitted: 2026-06-01
Accepted: 2026-10-15

# Modelos computacionales tiroideos específicos del paciente y simulaciones SIMIND Montecarlo para evaluar la exactitud de la dosimetría de $^{131}$I en hipertiroidismo

**Resumen:** El objetivo del estudio fue utilizar simulaciones de SIMIND Montecarlo (MC) junto con modelos computacionales tiroideos específicos de pacientes para evaluar la exactitud de la cuantificación de la actividad de 131I a partir de imágenes planares y los cálculos de dosimetría tiroidea en la terapia radiofarmacéutica con [131I] yoduro de sodio para hipertiroidismo. La metodología integra dos componentes: (i) modelos computacionales tiroideos específicos de pacientes con bocios grande y mediano, generados mediante el procesamiento de tomografías computadas de pacientes con el software 3D Slicer; y (ii) una cámara gama virtual creada con SIMIND MC. Con la cámara gama Picker Prism 2000 XP modelada se adquirieron imágenes planares de los modelos computacionales tiroideos específicos de los pacientes, en los cuales se asignó una actividad predefinida de 1,665 MBq al volumen tiroideo, utilizando un colimador de alta energía y una distancia tiroides-detector de 5 cm, como condiciones de adquisición de imágenes representativas de la clínica. Se utilizaron los mismos parámetros para simular imágenes planares del fantoma de referencia Zubal y una fuente de calibración para cuantificación. Los cálculos dosimétricos se basaron en un modelo de biodistribución monocompartimental de 131I, asumiendo un tiempo post- administración de 24 horas y un tiempo de eliminación efectivo de 5,5 días. Como resultado, se implementaron con éxito dos modelos computacionales tiroideos para pacientes con bocio, obteniendo imágenes de gamagrafía tiroidea realistas mediante SIMIND MC. La actividad tiroidea se cuantificó con un error del 3% para el fantoma Zubal y ≤0,4% para los modelos computacionales específicos de los pacientes, que se propagaron sin modificación a la dosis absorbida. Se verificó que la dosis absorbida por autoirradiación en la tiroides depende fuertemente de la masa tiroidea, siendo los valores de dosis para bocio de tamaño mediano el doble que para bocio grande, y varia ligeramente con la naturaleza del modelo computacional. El trabajo ilustra la utilidad de las simulaciones SIMIND MC junto con los modelos computacionales tiroideos para estimar la exactitud de los cálculos dosimétricos que podrían surgir en un entorno clínico real y la influencia de los parámetros de adquisición de imágenes y la masa tiroidea en la exactitud del cálculo.

**Palabras clave:** SIMIND MC, modelo computacional específico del paciente, bocio, dosis absorbida en tiroides.

SBPR

Copyright © 2026 Authors.

OPEN ACCESS

CC BY

## 1. INTRODUCTION

Iodine-131 therapy is one of the many therapeutic options available for benign thyroid diseases. Alternatives to radioiodine therapy are surgical resection in the form of hemi or total thyroidectomy and anti-thyroid drugs (ATDs) such as methimazole or propylthiouracil [1]. Radioiodine therapy (RIT) for benign thyroid diseases is based on the administration of [$^{131}$I] sodium iodide to the patients; this is taken up by the thyroid gland via sodium/iodide symporters, following the same biochemical pathways as stable iodine. Three main [$^{131}$I] sodium iodide prescription strategies coexist in clinical practice: fixed-activity methods, which administer a standard activity (370-740 MBq) regardless of individual patient characteristics; mass-based methods, which calculate the activity per unit thyroid volume (in general 3.7-11.1 MBq of [$^{131}$I] sodium iodide per mL of thyroid tissue) [2]; and individualized dosimetry, which incorporates patient-specific radioiodine uptake and biokinetics to deliver a prescribed absorbed dose to the thyroid. The latter approach has the potential to optimize treatment efficacy while minimizing unnecessary radiation exposure. The desired thyroid dose depends on the therapeutic goal and the treatment strategy: typically, a dose of 100–150 Gy to the target area is advised for managing hyperthyroidism when the goal is to achieve euthyroidism, while a dose of 200–300 Gy is suggested for the complete ablation of the target region [3].

Pre-therapeutic dosimetry procedure consists in administering a small, non-therapeutic [$^{131}$I] sodium iodide activity and measuring the thyroid´s uptake of the activity at one or more time points after administration. According to standard operational protocols, time- activity data for the thyroid can be obtained by using a dedicated probe, planar or SPECT/CT images [3], with variable quantification accuracy depending on the acquisition modality. While SPECT/CT imaging is often recommended for dosimetry calculations, in several applications it is also possible to use methods based on planar gamma camera imaging [4]. A recent comparison between planar and SPECT images for activity quantification in



OPEN ACCESS

CC BY

iodine-131 scintigraphy of patients with malignant thyroid disease, found that planar imaging showed comparable or, under specific conditions, improved agreement with dose estimates than SPECT images [5].

SIMIND (Simulating Medical Imaging Nuclear Detectors) [6] is a Monte Carlo simulation code that describes a standard clinical SPECT camera which can be conveniently modified virtually for any form of SPECT imaging experimentation. The advantage of using SIMIND MC software is that it allows for a more thorough analysis of energy transfer and can be used to investigate the causes of image degradation in nuclear medicine (NM) scintillation camera systems. The detector, radioactive source, and phantom can all be configured by the user [7]. SIMIND MC was used to model different gamma cameras and SPECT instruments [8- 10], to investigate the quantitative accuracy of activity estimates in NM images [11- 13] and to estimate the accuracy assessment of image- based absorbed doses [14, 15]. However, its performance in patient-specific thyroid geometries for $^{131}$I planar dosimetry has not been systematically assessed.

The aim of this study was to use SIMIND MC simulations together with patient-specific thyroid computational models to assess the accuracy of thyroid dosimetry calculations derived from $^{131}$I planar images in cases of hyperthyroidism, assuming a simplified dosimetry scheme based on a single early time point at 24 hours post-administration. The accuracy will be assessed based on the difference between the activity/dose recovered via imaging and the ground truth values known from the simulations.

## 2. MATERIALS AND METHODS

### 2.1. Patient-specific thyroid computational models

Patient-specific thyroid computational models of big and medium goitre (with thyroid´s masses of 60 and 30 grams, respectively) were generated from clinical CT scans



OPEN ACCESS

of the neck region, with an isotropic voxel size of 0.0976 cm (in-plane pixel size and slice thickness). Thyroid segmentation was performed automatically using the Total Segmentator tool within 3D Slicer Image Computing software; given that the field of view was restricted to the neck region and the thyroid was clearly delineated, no manual correction of the segmentation was required. Since 3D Slicer assigns segment index values based on the order of segmentation, which may differ between phantoms, a remapping step was performed prior to format conversion: a Python script was used to reassign each anatomical structure to the fixed index values required by the SIMIND Zubal phantom framework (e.g., thyroid = 28, liver = 12, kidneys = 14). The remapped volume was then converted from 16-bit to 8-bit format using Fiji, as required by SIMIND for Zubal-type phantom handling. A calibration source phantom was obtained in the same way from a real CT scan of a cylindrical calibration source.

## 2.2. Configuration of virtual gamma camera

SIMIND MC code was used to model a Picker Prism 2000 XP gamma camera. The virtual gamma camera had previously been validated by Vitaller [16] and Calandrón [17], through routine quality control tests (intrinsic uniformity UFOV and CFOV, and extrinsic resolution) performed under conditions identical to those used in the clinical setting. The QC values obtained with the virtual clinical simulator were consistent with those expected by the manufacturer of the real gamma camera, thereby validating the modelized clinical simulator [18]. The virtual gamma camera was used to acquire planar images of the patient-specific thyroid computational models containing 1.665 MBq of $^{131}$I in the gland as ground-truth activity, using a high-energy collimator and a distance thyroid/detector of 5 cm, like a real clinical setting. The choice of 1.665 MBq of [$^{131}$I] sodium iodide as reference thyroid activity reflects a clinical scenario of pre-therapeutic dosimetry in which a tracer activity of [$^{131}$I] sodium iodide (3.7 MBq) is administered [3] and, 24 hours post-administration, 45% of the activity is incorporated into the gland, a typical uptake value in hyperthyroid patients [19].



OPEN ACCESS

The same acquisition parameters and thyroid ground-truth activity were used to simulate planar images of a reference thyroid Zubal phantom.

For the aim of $^{131}$I activity quantification, and replicating the procedure used in clinical practice to obtain a calibration factor (CF), a calibration source with spherical geometry and a known activity of 1.08 MBq was modeled, and a simulated planar image was acquired—under the aforementioned acquisition conditions—, in order to convert the number of counts in the region of interest (ROI) into units of activity. It should be noted that, since SIMIND Monte Carlo simulations model photon transport independently, actual detector hardware effects—such as dead time, pulse pile-up, and electronic saturation—are absent by design. Consequently, the relationship between counts and activity is linear across the activity range used in this study (1.08–1.665 MBq); therefore, no linearity correction of the CF was required for thyroid activity quantification.

## 2.3. Activity quantification

Quantification of $^{131}$I activity in the simulated images was performed in Fiji using the Raw Integrated Density value. The thyroid ROI was manually delineated using a rectangular tool, based on the known butterfly-like anatomy of the thyroid gland. Different rectangle sizes were tested—including larger or smaller background areas—without resulting in significant differences in the count values. The activity recovered in the thyroid was calculated as:

$$A_{recovered}\,[MBq] = (Counts_{thyroid}\,[counts] \times Activity_{calibration\ source}\,[MBq]) / Counts_{calibration\ source}\,[MBq] \qquad Eq.\ 1$$

where $A_{recovered}$ is the thyroid´s activity that emerges from the analysis of the image, $Counts_{thyroid}$ is the Raw Integrated Density value in the thyroid´s ROI, $Activity_{calibration\ source}$ is 1.08 MBq and $Counts_{calibration\ source}$ is the Raw Integrated Density value in the calibration source´s ROI.

Raw count rates, without any further correction, were used for activity quantification, given that deleterious image effects inherent to real gamma cameras were either absent or minimized in this computational study. The contribution of scattered radiation was



OPEN ACCESS

minimized by applying an energy window centered on the 364 keV photopeak of $^{131}I$, in accordance with standard clinical acquisition protocols. Background radiation outside the thyroid region of interest (ROI) was verified to be negligible, given the absence of activity in surrounding structures in the simulation. Detector dead time and uniformity corrections are not applicable to Monte Carlo simulations, as these are hardware-dependent effects that are, by design, absent in SIMIND.

## 2.4. Absorbed dose calculations

Dosimetry calculations were performed using the single-uptake biokinetic model, a simplified method that is seeing a resurgence among multi-time-point models, as it reduces the number of hospital visits [4]. The model involves using an effective half-life $T_{eff}$ for radioiodide of 5.5 days or disease specific half-lives if they are known to be more representative for the respective patient population [3]. In this study, we use a half-life of 5.5 days for [$^{131}I$] sodium iodide as it is characteristic of Graves´disease (GD) [20], the specific hyperthyrodic condition that we have modeled in this article. Under these suppositions and considering a monoexponential behavior in the radioiodine elimination, the cumulated activity Ã in the thyroid can be calculated as:

$$\tilde{A}\ [MBq.d] = (A_0\ [MBq] \times T_{eff}\ [d]) / ln\ 2 \qquad Eq.\ 2$$

where $A_0$ is the initial thyroid activity, that can be obtained from:

$$A_0\ [MBq] = A_{24\ h}\ [MBq] \times exp\ (ln\ 2\ /\ T_{eff}\ [d]) \qquad Eq.\ 3$$

where $A_{24\ h}$ is $A_{recovered.}$

For the thyroid gland, as both source and target regions are the same (self-irradiation), it can be demonstrated [3] that the absorbed dose can be calculated as:

$$D\ [Gy] = \tilde{A}\ [MBq.d] \times \bar{E}\ [Gy.g/MBq.d]) / M\ [g] \qquad Eq.\ 4$$



OPEN ACCESS

CC BY

where a constant value of 2.808 Gy.g/(MBq.d) is used for $\bar{E}$, the mean absorbed dose in the thyroid gland per $^{131}$I disintegration [3] and $M$ is the thyroid mass. $\bar{E}$ is calculated by summing the absorbed energy from all $^{131}$I emissions, assuming thyroid self-irradiation: all energy from $\beta^-$ emissions is absorbed by the gland and only 3% of the emitted gamma energy is absorbed (a scenario corresponding to a 20 g thyroid). The use of this constant value for $\bar{E}$ typically introduces an error of ≤5% for masses M ≤90 g and yields results with adequate accuracy for the majority of patients [3].

The accuracy of the estimated $^{131}$I absorbed doses was assessed by comparison to the ground truth absorbed doses $D_{ground\ truth}$ that were obtained by performing the same calculations directly for the ground truth activity assigned to the thyroid computational models (1.665 MBq) and a mass M of 30 or 60 grams, depending if medium- or big-goitre were considered. The absorbed dose percent error (%) was calculated from:

$$D\ percent\ error\ [\%] = 100 \times (D\ [Gy] - D_{ground\ truth}\ [Gy]) / D_{ground\ truth}\ [Gy] \qquad Eq.\ 5$$

## 3. RESULTS AND DISCUSSIONS

### 3.1. Patient- specific thyroid computational models

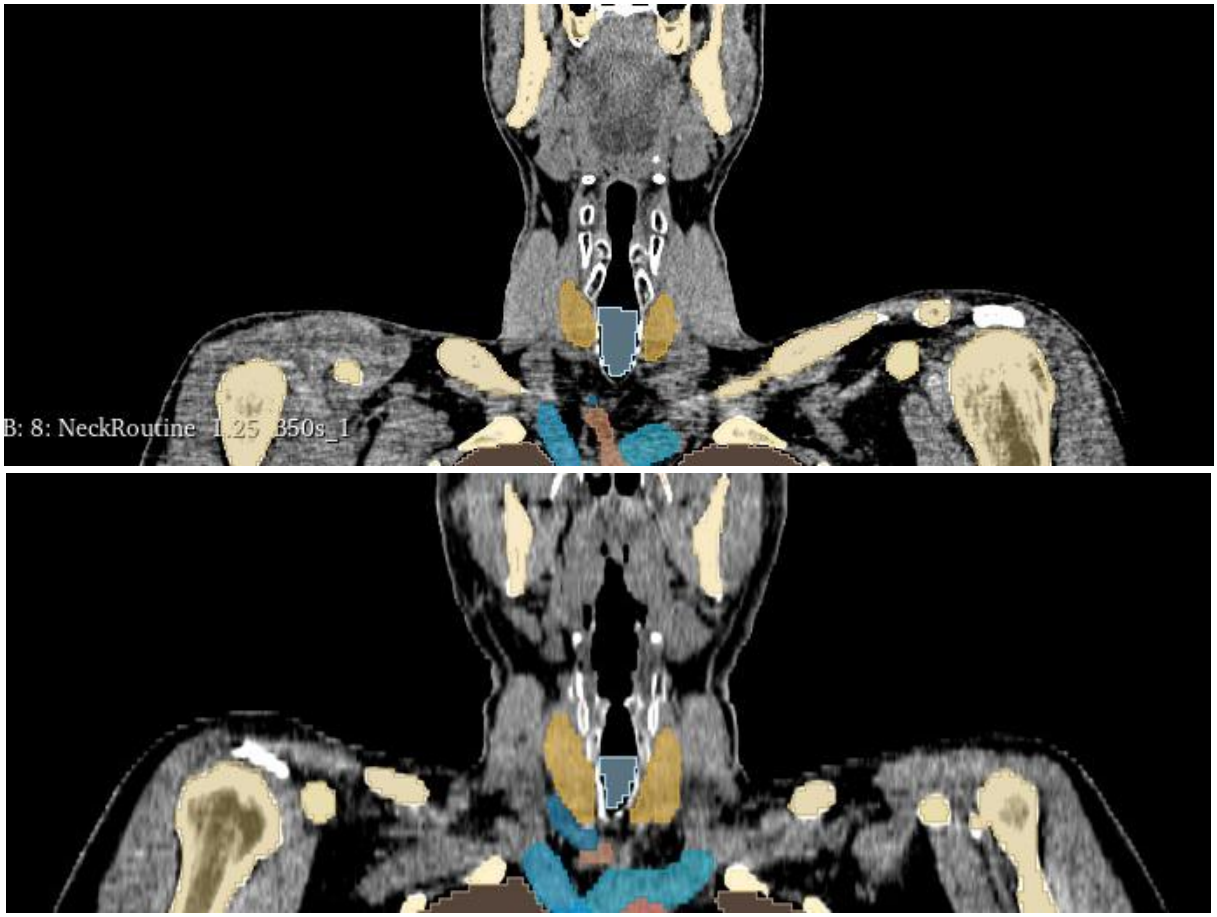
The patient-specific thyroid computational models of two different goitre patients have been successfully implemented. In Fig. 1, coronal views of the obtained patient specific medium- and big-goitre computational models are displayed.



OPEN ACCESS

CC BY

**Figure 1:** Images showing a coronal view of patient-specific thyroid computational models (top-medium goitre, bottom- big goitre). The orange structures correspond to the thyroid lobes.




Source: Screenshots from 3D Slicer coronal views.

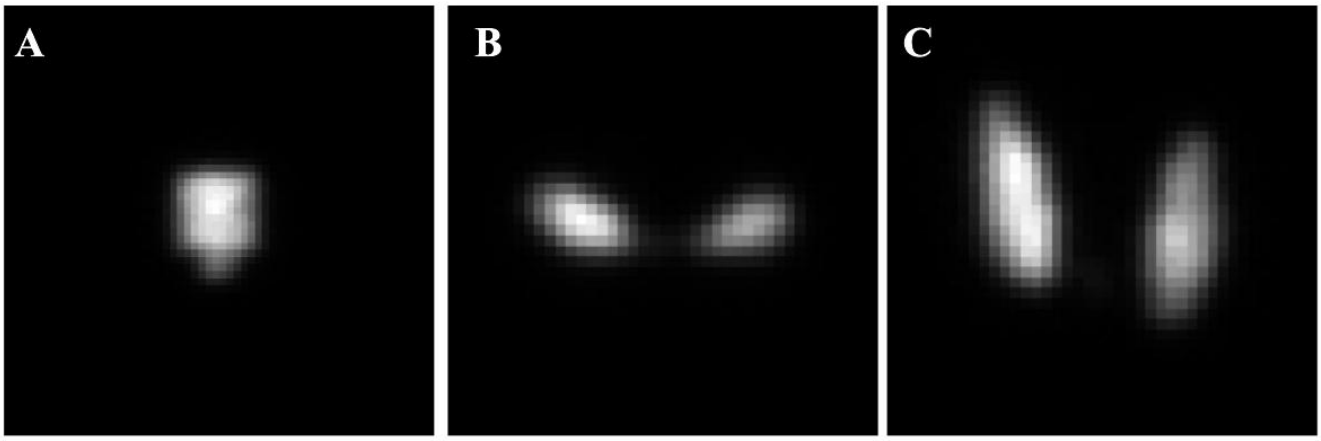
## 3.2. Activity quantification and dose calculation from simulated planar images

Fig. 2 shows simulated planar images obtained with the proposed methodological framework, where the cylindrical shape and the butterfly- shaped thyroid can be seen for the calibration source (A) and the goitre models (B and C).



OPEN ACCESS

**Figure 2:** Simulated planar images of: A. Calibration source; B. Patient-specific thyroid computational model with medium goitre; C. Patient- specific thyroid computational model with big goitre.




Source: Screenshots from FIJI image display.

The measured integrated counts within the thyroid ROIs, obtained using Fiji software, were corrected using the CF (MBq/counts). The activity quantified in the thyroid gland, the correspondent cumulated activity calculated from Eq. 2 and Eq. 3, the thyroid absorbed dose calculated from Eq. 4 and the associated percentage error are presented in Table 1 for the patient- specific thyroid computational models, and the Zubal reference phantom, together with the ground truth values corresponding to the modeled clinical scenario.

**Table 1:** Activity quantified in the thyroid gland, cumulated activity, thyroid absorbed dose and percentage error for the patient- specific thyroid computational models, and the Zubal phantom, together with the ground truth values corresponding to the modeled clinical scenario. Uncertainties in $A_{24h}$ are statistical deviations from the simulations, and uncertainties in Ã and D correspond to uncertainty propagation.

| Clinical scenario | $A_{24h}$ [MBq] | Ã [MBq. day] | Thyroid mass (g) | D [Gy] | D percent error [%] |
|---|---|---|---|---|---|
| Ground truth situation | 1.665 | 14.986 | 30 | 1.402 | - |
| | | | 60 | 0.701 | - |
| Zubal Thyroid | 1.61(8) FIJI | 14.5(7) | 30 | 1,35(7) | 3 |
| | | | 60 | 0.68(3) | 3 |
| Patient- specific thyroid computational model, medium goitre | 1.670(5) FIJI | 15.04(5) | 30 | 1.407(4) | 0.4 |
| Patient- specific thyroid computational model, big goitre | 1.664(3) FIJI | 14.98(3) | 60 | 0.701(2) | 0 |



OPEN ACCESS
CC BY

The maximum activity quantification error was 3% for the thyroid of the Zubal reference phantom, that propagates without modification to the cumulated activity and the thyroid absorbed dose. This finding is related to the linearity of the dose-activity relationship for a fixed mass in the single-point biokinetic model analyzed in this article (Eq. 2 – Eq. 4), implying that the relative error in the dose tracks the relative error in the activity. From a clinical perspective, the error is small compared to the spread of thyroid absorbed dose values reported in patients with GD, as verified in a recent study involving a cohort of 15 patients, in which a 2.5-fold difference in absorbed thyroid dose was observed, with a mean dose coefficient of 653 mGy/MBq [21]. The results suggested that, under the assumptions of this model, planar image-based quantification may provide a substantially closer estimate of the thyroid absorbed dose than using population-average values.

It is worth highlighting the strong dependence of the dose absorbed by the thyroid on the gland's mass, that in this model is inversely proportional, for a fixed cumulated activity. In this regard, it should be noted that standard dosimetry—based on pre-calculated S-values, and assuming an average mass for the target organ—cannot be applied to patients with hyperthyroidism, given the interindividual variation in gland mass, that ranges 10.5-86.8 g, with a mean of 25.3 g [22]. In this regard, estimating thyroid mass should not be overlooked during the clinical planning of the therapy.

## 3.3. Significance of the results obtained

The study is entirely computational; the modeling and simulation were designed to reproduce a realistic clinical scenario involving a patient with hyperthyroidism treated with radioiodine and undergoing pre-therapeutic dosimetry calculations.

Regarding the validity of the virtual gamma camera, it was based on quality control test results performed using reference radioactive source geometries, that showed excellent correlation with the characteristic values of the real medical device. Nevertheless, no validation was performed using planar images of real patients acquired by the device, which limits the scope of the obtained results.

 Copyright © 2026 Authors

OPEN ACCESS

With respect to the computational patient models, only two specific phantoms (medium and big goitre) were evaluated; therefore, the results cannot be extrapolated to other clinical scenarios (e.g., thyroids with highly atypical geometry or retrosternal goiter) where specific phantom characteristics could have a greater impact. Finally, the use of the fixed-[$^{131}$I] sodium iodide halftime typical of GD circumscribes the study to this case of hyperthyroidism, without considering, in this first approach, the biokinetic variability between patients, that is reported to be of at least 27 % [20].

Regarding the 3% dosimetry error reported in this study, it reflects only the uncertainty associated with activity quantification from planar images under the simulated conditions and should not be interpreted as the total uncertainty of the dosimetry calculation. As described in the EANM practical guidance on uncertainty analysis for molecular radiotherapy absorbed dose calculations [23], the full dosimetry uncertainty chain encompasses additional clinically relevant sources, including thyroid mass estimation, ROI delineation, individual variability in radioiodine biokinetics, patient positioning, and the S-factor. Among these, thyroid mass estimation and biokinetic variability are expected to be the dominant contributors to overall dosimetry uncertainty in clinical practice, as the absorbed dose is strongly dependent on both the mass of the gland and the individual effective half-life of radioiodine. The present study isolates and quantifies the contribution of image-based activity quantification to this uncertainty chain, within the assumptions of a fixed monoexponential biokinetic model.

Besides the aforementioned limitations, which restrict the direct extrapolation of the numerical results obtained in the virtual scenario to the physical world, this type of study allows for the identification of significant trends, such as the feasibility of performing pre-therapeutic dosimetry calculations from planar images using a one- uptake biokinetic model, the suitability of the Zubal phantom for this type of exploratory studies, and the importance of knowing the patient's thyroid mass for dosimetry planning. Finally, it is worth noting that computational studies in NM allow for the investigation of multiple clinical scenarios



OPEN ACCESS

CC BY

without exposing patients to ionizing radiation, identifying operational parameters or optimized practices that pave the way for more precise, high-quality healthcare.

## 4. CONCLUSIONS

This study illustrates the utility of SIMIND MC simulations together with thyroid computational models to estimate the accuracy of a dosimetry calculation that could emerge under clinically representative imaging conditions.

The research demonstrated that it is possible to quantify thyroid activity from planar images and calculate the absorbed dose in the thyroid with adequate accuracy across the three anthropomorphic computational models, using a single-point biokinetic model with a fixed radioiodine half-life of 5.5 days. The results reinforce the applicability of pretherapeutic dosimetry planification in RIT of hyperthyroidism. For the activity quantification approach investigated here, the two created patient-specific geometries did not provide a measurable improvement in accuracy over the Zubal reference phantom.

The results illustrate the marked dependence of the thyroid absorbed dose on the mass of the gland, not only due to the definition of absorbed dose itself but also because of the wide variation in thyroid volume among patients with hyperthyroidism, making it virtually impossible to perform dosimetry without an accurate estimate of the patient-specific mass.

## FUNDING

This research did not receive any specific grant from funding agencies in the public, commercial, or not-for-profit sectors.



OPEN ACCESS

CC BY

## CONTRIBUTORSHIP

**Conceptualization**: CYC

**Data curation:** EHA

**Formal analysis:** EHA, LHI, CYC

**Investigation**: EHA, LHI

**Methodology:** EHA, LHI, CYC

**Supervision:** LHI, CYC

**Writing – original draft:** CYC

**Writing – review and editing**: EHA, CYC

## CONFLICT OF INTEREST

All authors declare that they have no conflicts of interest.

## DATA AVAILABILITY STATEMENT

Derived data supporting the conclusions of this study are available upon request from the corresponding author.

## REFERENCES

[1] R ROSS, D. S.; BURCH, H. B.; COOPER, D. S. et al. 2016 American Thyroid Association guidelines for diagnosis and management of hyperthyroidism and other causes of thyrotoxicosis. **Thyroid**, New Rochelle, NY, US, v. 26, n. 10, p. 1343-1421, 2016



OPEN ACCESS

CC BY

[2] European Association of Nuclear Medicine. European Nuclear Medicine Guide, Chapter 5.2, Na[$^{131}$I]I for Thyroid Benign Diseases. Disponível em: https://nucmed-guide.app/chapter/302. Acesso em: 1 jun. 2026.

[3] HÄNSCHEID, H.; CANZI, C.; ESCHNER, W. et al. EANM Dosimetry Committee series on standard operational procedures for pre-therapeutic dosimetry II: Dosimetry prior to radioiodine therapy of benign thyroid diseases. **European Journal of Nuclear Medicine and Molecular Imaging**, London, UK, v. 40, n. 7, p. 1126-1134, 2013.

[4] GEAR, J.; STOKKE, C.; TERWINGHE, C.; GNESIN, S. et al. EANM enabling guide: how to improve the accessibility of clinical dosimetry. **European Journal of Nuclear Medicine and Molecular Imaging**, London, UK, v. 50, n. 7, p. 1861-1868, 2023.

[5] IIZUKA, Y.; KATAGIRI, T.; INOUE, M. et al. Comparison between planar and single-photon computed tomography images for radiation intensity quantification in iodine-131 scintigraphy. **Scientific Reports**, London, UK, v. 11, n. 1, 21858, 2021.

[6] LJUNGBERG, M. **The SIMIND Monte Carlo Program Version 6.2**. Lund University, Medical Radiation Physics, Department of Clinical Sciences, Lund, Sweden, 2020.

[7] CHATZISAVVAS, N.; PRINIOTAKIS, G.; PAPOUTSIDAKIS, M. et al. Monte Carlo computational software and methods in radiation dosimetry. **Annals of Emerging Technologies in Computing (AETiC)**, London, UK, v. 5, n. 3, p. 36-51, 2021.

[8] ORAMAS POLO, I. Simulation of the functioning of a gamma camera using Monte Carlo method. **Revista de Física Médica**, Madrid, Spain, v. 15, n. 1, p. 21-28, 2014.

[9] MORPHIS, M.; VAN STADEN, J. A.; DU RAAN, H.; LJUNGBERG, M. Validation of a SIMIND Monte Carlo modelled gamma camera for Iodine-123 and Iodine-131 imaging. **Heliyon**, London, UK, v. 7, n. 6, e07196, 2021.

[10] DE LA CRUZ MARIN, J. L.; CHAIN, C. Y.; ILLANES, L. H. Modelo computacional de una cámara gama como simulador de imágenes clínicas. **Anales AFA**, Buenos Aires, Argentina, v. 36, n. 2, p. 1-1, 2025.

[11] DAISAKI, H.; KUBOTA, C.; ISHIKAWA, K. et al. Validation of Quantitative Accuracy and Variability in $^{177}$Lu Imaging Using Monte Carlo Simulation. **Nihon Hoshasen Gijutsu Gakkai Zasshi**, Kyoto, Japan, v. 80, n. 6, p. 593-604, 2024.

[12] DE LA CRUZ MARIN, J. L.; CHAIN, C. Y.; ILLANES, L. H. Exactitud en la cuantificación de la actividad de $^{131}$I a partir de imágenes SPECT: un estudio SIMIND monte carlo. **Anales AFA**, Buenos Aires, Argentina, v. 37, n. 1, p. 1-5, 2026.



OPEN ACCESS

CC BY

[13] RAMONAHENG, K.; VAN STADEN, J. A.; DU RAAN, H. The effect of calibration factors and recovery coefficients on $^{177}$Lu SPECT activity quantification accuracy: a Monte Carlo study. **EJNMMI Physics**, London, UK, v. 8, p. 27, 2021.

[14] MORPHIS, M.; VAN STADEN, J. A.; DU RAAN, H.; LJUNGBERG, M.; SJÖGREEN GLEISNER, K. Accuracy of patient-specific $^{131}$I dosimetry using hybrid whole-body planar-SPECT/CT $^{123}$I and $^{131}$I imaging. **EJNMMI Physics**, London, UK, v. 11, p. 50, 2024.

[15] LJUNGBERG, M.; DEWARAJA, Y. K. The use of Monte Carlo simulations to evaluate image-based absorbed dose calculation procedures. In: ZAIDI, H. (Ed.). **Monte Carlo Calculations in Nuclear Medicine (Second Edition) Therapeutic applications**, Bristol, UK: IOP Publishing, 2022. p. 20.1-20.26. ISBN 978-0-7503-2692-6.

[16] VITALLER, M. J. Evaluación de métodos de cuantificación de actividad de 131 I a partir de imágenes bidimensionales: Análisis comparativo utilizando SIMIND MC. Doctoral dissertation. Universidad Nacional de La Plata, La Plata, Argentina, 2025.

[17] CALANDRÓN, V. M. Utilidad de las simulaciones basadas en Montecarlo para la implementación de cálculos dosimétricos en tratamientos de hipertiroidismo Doctoral dissertation. Universidad Nacional de La Plata, La Plata, Argentina, 2026.

[18] VITALLER, M. J.; AMAN, E.; DE LA CRUZ MARIN, J. L.; CALANDRÓN, V. M.; CHAIN, C. Y.; ILLANES, L. H. Computational simulation of nuclear medicine images in patients with thyroid diseases. In: Memorias del Simposio de Modelado y Simulación (SIMS 2026)-JAIIO 55 2026, La Plata, Argentina. **Memorias: La Plata, Argentina: Sociedad Argentina de Informática e Investigación Operativa (SADIO)**, 2026.

[19] FRANKLYN, J.; SHEPHARD, M. Evaluation of thyroid function in health and disease. Disponível em: https://www.endotext.org/. Acesso em: 15 set. 2026.

[20] KOBE, C.; ESCHNER, W.; WILD, M. et al. Radioiodine therapy of benign thyroid disorders: what are the effective thyroidal half-life and uptake of 131I?. **Nuclear Medicine Communications**, London, UK, v. 31, n. 3, p. 201-205, 2010.

[21] ANDERSSON, M.; MATTSSON, S. Improved Patient Dosimetry at Radioiodine Therapy by Combining the ICRP Compartment Model and the EANM Pre-Therapeutic Standard Procedure for Benign Thyroid Diseases. **Frontiers in Endocrinology**, Lausanne, Switzerland, v. 12, 634955, 2021.

[22] PÉREZ, J. M.; ORELLANA SALAS, A.; GUARDIOLA, Y. S. Comparación dosimétrica entre actividad fija y actividad individualizada en el tratamiento de la



OPEN ACCESS

enfermedad de Graves con I-131. **Revista de Física Médica**, Madrid, Spain, v. 14, n. 2, p. 123-130, 2013.

[23] GEAR, J. I.; COX, M. G.; GUSTAFSSON, J. et al. EANM practical guidance on uncertainty analysis for molecular radiotherapy absorbed dose calculations. **European Journal of Nuclear Medicine and Molecular Imaging**, London, UK, v. 45, n. 13, p. 2456-2474, 2018.

## LICENSE

This article is licensed under a Creative Commons Attribution 4.0 International License, which permits use, sharing, adaptation, distribution and reproduction in any medium or format, as long as you give appropriate credit to the original author(s) and the source, provide a link to the Creative Commons license, and indicate if changes were made. The images or other third-party material in this article are included in the article's Creative Commons license, unless indicated otherwise in a credit line to the material.
To view a copy of this license, visit http://creativecommons.org/ licenses/by/4.0/.